



Prognosis and progression of phagocytic regulatory factor-related gene combinations in clear cell renal cell carcinoma (ccRCC)

Ruihai Xiao^{1#}, Zepeng Luo^{2#}, Hongwei Huang², Yingqun Yin¹

¹Department of Urology, Jiangxi Academy of Medical Science, Nanchang University, Nanchang, China; ²Department of Urology, The Second Affiliated Hospital, Jiangxi Medical College, Nanchang University, Nanchang, China

Contributions: (I) Conception and design: H Rui, Z Luo; (II) Administrative support: Q Yin; (III) Provision of study materials or patients: H Huang; (IV) Collection and assembly of data: R Xiao, Y Yin; (V) Data analysis and interpretation: R Hai, Z Luo, H Huang; (VI) Manuscript writing: All authors; (VII) Final approval of manuscript: All authors.

[#]These authors contributed equally to this work as co-first authors.

Correspondence to: Yingqun Yin, MM. Department of Urology, Hospital of Nanchang University, Nanchang University, No. 461 Bayi Road, Nanchang 330006, China. Email: 619062360@qq.com.

Background: Developing signatures based on specific characteristics to predict prognosis has become a research hotspot in oncology. However, the prognostic value of phagocytosis regulators in clear cell renal cell carcinoma (ccRCC) remains unclear. The aim of the present study was to investigate the prognostic significance of phagocytosis regulators in ccRCC by constructing a prognostic model related to phagocytosis regulators, and to use this model to evaluate the prognosis and treatment effects in ccRCC patients.

Methods: Firstly, kidney renal clear cell carcinoma (KIRC) transcriptome data (RNA-Seq) and clinical data were downloaded from The Cancer Genome Atlas (TCGA) database. Based on literatures PMID 34497417 and PMID 30397336, 167 of the 173 phagocytosis regulator genes collected in the literature were expressed in TCGA-KIRC. The relationship between these regulators and macrophages was revealed through single-sample gene set enrichment analysis (ssGSEA), and their biological and pathway involvements were further analyzed using Gene Ontology (GO) and Kyoto Encyclopedia of Genes and Genomes (KEGG) enrichment analyses. Univariate Cox regression analysis and the least absolute shrinkage and selection operator (LASSO) method were employed to further select phagocytosis regulators with prognostic potential, leading to the construction of a prognostic regression model. Additionally, univariate and multivariate Cox regression analyses were conducted to confirm the prognostic independence of genes associated with phagocytosis regulators. Finally, the relationship between phagocytosis regulator-related genes and patients' immune microenvironments and immunotherapy responses was explored.

Results: We have constructed a prognostic model of a combination of genes associated with phagocytosis regulators using LASSO Cox regression analysis of genes, and our combined model was shown to be an independent prognostic factor. The model had optimal performance in predicting long-term survival. Clinical features were significantly correlated with phagocytosis regulatory gene scores. Tumors with higher levels of grade and stage were more prone to have higher phagocytosis regulatory genes. And our study suggests that phagocytosis regulatory genes do not play an ideal role in predicting the efficacy of immunotherapy in patients.

Conclusions: We have constructed a prognostic model using a combination of genes associated with phagocytosis regulators, providing new insights into the prognosis and progression of ccRCC.

Keywords: Clear cell renal cell carcinoma (ccRCC); phagocytosis regulators; macrophages; prognostic model

Submitted Jan 18, 2024. Accepted for publication Jun 21, 2024. Published online Sep 27, 2024.

doi: 10.21037/tcr-24-139

View this article at: <https://dx.doi.org/10.21037/tcr-24-139>

Introduction

Globally, renal cell carcinoma (RCC) accounts for more than 2% of neoplasms in humans worldwide, with the incidence and mortality persistently increasing (1). Gene signatures based on specific characteristic-related to predict prognosis have become a hotspot in cancer research (2-4). The prognostic value of phagocytosis regulators in clear RCC is unclear. Immunotherapy is considered the most promising method to overcome cancer, and macrophages are promising targets in future cancer immunotherapy (5). Phagocytic cells can eliminate cancer cells through phagocytosis, and 173 potential macrophage-regulated genes were obtained by Kamber *et al.* (6,7). Our study investigated the relationship between phagocytosis regulator gene expression and prognosis in clear cell RCC (ccRCC) patients in the Cancer Genome Atlas Kidney Renal Clear Cell Carcinoma (TCGA-KIRC) database. Inflammatory cells are a key component in cancer ecology (8). The macrophages are the main component of leukocyte infiltration, and there are different numbers of macrophages in all tumors (9). The macrophages are the key to promoting tumor inflammation. Tumor-associated macrophages (TAMs) promote tumor progression at various levels, including promoting genetic instability, cultivating cancer stem cells, paving the way for metastasis, and taming adaptive protective immunity. TAM expression triggers T cell activation of checkpoints and is the target of checkpoint blockade immunotherapy. Macrophage-centric therapies include strategies to prevent tumor

recruitment and survival; anti-tumor function reeducation, M1-like mode; tumor-directed monoclonal antibodies that can cause extracellular killing or phagocytosis of cancer cells (10). Monoclonal antibody therapy targeting tumor antigens largely drives the elimination of cancer cells by triggering macrophage phagocytosis of cancer cells. However, the mechanisms by which cancer cells escape phagocytosis are poorly understood. As a 'Do not eat me' signal, CD47 is a known regulator that protects cells from phagocytosis by binding to and activating its receptor SIPRA on macrophages (11). Identifying and characterizing phagocytosis regulators is vital for describing the mechanism of phagocytosis in tumors. Two genome-wide CRISPR articles (6,7) have identified some important phagocytosis regulators. However, the effects of these regulators on tumorigenesis and progression in ccRCC have not been studied. To this end, using data from TCGA, we employed the Cox regression model to evaluate the prognostic relevance of phagocytosis regulator genes in patients with ccRCC. By applying the least absolute shrinkage and selection operator (LASSO) regression, we were able to select the most significant predictors from a vast pool of potential biomarkers. These selected candidates were then used to compute a signature score that assesses patient prognosis and treatment outcomes. This analysis has provided new insights into the role of phagocytosis regulators in the progression and prognosis of ccRCC. We present this article in accordance with the TRIPOD reporting checklist (available at <https://tcr.amegroups.com/article/view/10.21037/tcr-24-139/rc>).

Highlight box

Key findings

- The prognostic model of a combination of genes associated with phagocytosis regulators had optimal performance in predicting long-term survival.

What is known and what is new?

- Immunotherapy is considered the most promising method to overcome cancer, and macrophages are promising targets in future cancer immunotherapy.
- We explored phagocytosis regulators that could effectively assess clinical prognosis in clear renal cell carcinoma. And phagocytosis regulator genes are closely associated with immune infiltration, phagocytic immune checkpoints and inflammatory factors.

What is the implication, and what should change now?

- In clear renal cell carcinoma, phagocytosis regulators have important prognostic value.

Methods

Data collection

The study was conducted in accordance with the Declaration of Helsinki (as revised in 2013).

TCGA ccRCC

TCGA database of kidney renal clear cell carcinoma (KIRC) transcriptome data (RNA-Seq) and clinical information data were obtained through Bioconductor package TCGA bio links (12). RNA-Seq data normalized fragments per kilobase of exon model per million mapped fragments (FPKM) expression profile of tumor samples [526] and normal samples [72]. The clinical information included the overall survival time, survival status, and other clinical phenotype data of KIRC patients, including age, gender, tumor grade, tumor stage, and other information (*Table 1*).

Table 1 Clinical information of patients with TCGA-KIRC tumors

Characteristics	Type	Patients
Gender	Female	184
	Male	342
Stage	I	263
	II	56
	III	122
	IV	82
	NA	3
Grade	G1	14
	G2	224
	G3	205
	G4	75
	NA	8
Age, years	≥60	261
	<60	265

TCGA-KIRC, The Cancer Genome Atlas Kidney Renal Clear Cell Carcinoma; NA, not application.

GEO ccRCC

GEO resource platform (<https://www.ncbi.nlm.nih.gov/gds>) was used to download a set of renal clear cell carcinoma data (GSE167573, including 62 tumor samples) including log2-transformed TPM (transcripts per million). In addition, transcriptome expression profiles and tumor clinical information (Table S1) were used to validate the analysis.

Feature collection of 28 types of immune cells

The characteristic gene set of 28 immune cells was derived from Clyde *et al.* (13).

Immune subtypes of TCGA tumors

The immune subtypes of TCGA tumors were derived from Thorsson *et al.* (14), and TCGA-KIRC included a total of 6 subtypes C1-C6 (Table S2).

Phagocytosis regulators

A total of 90 and 85 phagocytosis-related regulator genes were collected from literature Kamber *et al.* (6) and Haney *et al.* (7), respectively. The union of the two sets of 173 genes was used as phagocytosis regulators combined and used for subsequent analysis.

Research methods

Technical route

ssGSEA calculates an immune cell enrichment score

Through the ssGSEA method of Bioconductor package gene set variation analysis (GSVA) (15), we used the log₂(FPKM+1) transformed TCGA-KIRC expression profile and 28 immune cell signature gene sets as the input of ssGSEA and calculated each sample in each immune cell ssGSEA enrichment score.

GO/KEGG functional enrichment analysis

The GO/KEGG functional enrichment analysis was performed on the collected phagocytosis regulators using the clusterProfiler (16) of the Bioconductor package, and the functional enrichment was considered to be statistically significant when the calculated result $P < 0.05$ (without multiple test correction).

Differential analysis of tumor and normal samples

Based on the expression data of log₂ (FPKM+1) normalized by TCGA-KIRC, we evaluated the model using ImFit, the linear fitting method of limma (17). In addition, we calculated the difference between ccRCC and normal samples using the eBayes method. When fold-change > 1.5 and FDR < 0.05 , the gene expression was significantly different.

Construction and evaluation of phagocytosis regulator genes

First, using R package survival, Cox regression analysis was performed on differentially expressed phagocytosis regulators based on TCGA-KIRC tumor expression profile data, survival time, and survival status (18) to determine the hazard ratio (HR) of genes and significant prognosis, and screened genes with significant $P < 0.05$ as candidate prognostic factors. Subsequently, R package glmnet (19) was used to perform LASSO regression on the candidate prognostic factors, and the factors that significantly impacted survival were selected as phagocytosis regulators. Next, the regression coefficients corresponding to each factor were calculated. Then, the weighted sum of the expression of each prognostic factor and LASSO regression coefficient is used as the sigScore (Signature Score) of each sample, and the calculation formula is as follows: $sigScore = \sum exp_i \times coef_i$, where i represents the prognostic factor, and exp represents each prognosis. The expression level of the factor, and $coef$ represents the LASSO regression coefficient.

To evaluate the correlation between phagocytosis regulator genes and prognosis, the samples were divided

into high-risk and low-risk groups according to the median value of sigScore. Then the survival and log-rank test models were constructed using the R package survival, and then survminer (19) demonstrated the Kaplan-Meier survival curve and the significance of the difference between the two groups. Simultaneously, R package timeROC (20) was used to construct the time-dependent receiver operating characteristic (ROC) curve of sigScore to evaluate the performance of phagocytosis regulators.

Finally, univariate and multivariate Cox regression models were used to evaluate whether phagocytosis regulatory factors could be used as independent prognostic factors, and R-package forest model (21) was used to display the forest map of regression analysis.

Immune microenvironment

ESTIMATE (Estimating STromal and Immune cells in Malignant Tumor tissues using Expression data) can use the unique properties of tumor transcriptional profiles to infer the content of immune cells and stromal cells as well as tumor purity (22). In addition, many algorithms can infer the proportion or score of immune cells in the tumor microenvironment from tumor expression profiles. To this end, we evaluated different immune cell scores using ESTIMATE (23), EPIC (24), quanTIseq (25), and ssGSEA [evaluating 28 immune cells (24)] from R package IOBR (26), respectively.

Statistical analysis

All statistical analyses were performed by R software (<https://www.r-project.org>). The Mann-Whitney U test was used to compare the differences between two groups of samples when performing significant analysis between various values (expression level, infiltration ratio, etc.). In the plot presentation, where ns means $P > 0.05$, * means $P \leq 0.05$, ** means $P \leq 0.01$, *** means $P \leq 0.001$, and **** means $P \leq 0.0001$.

Results

Phagocytosis regulators are associated with macrophage activity and participate in the occurrence and development of renal clear cell carcinoma

Phagocytosis regulators are associated with macrophage activity

Through mapping, we found that 167 of the 173

phagocytosis regulator genes collected in the literature were expressed in TCGA-KIRC. Subsequently, to explore the association of phagocytosis regulators with macrophages, we calculated the macrophage enrichment score for each sample of TCGA-KIRC using the macrophage gene set and then calculated the enrichment score with each phagocytosis regulator (*Figure 1*). As a result, we found that many phagocytosis regulators were positively correlated with macrophage scores (*Figure 1A*), and macrophages could also significantly distinguish the expression abundance of phagocytosis regulators (*Figure 1B*).

Functional analysis of phagocytosis regulators

We conducted a functional enrichment analysis of 167 phagocytosis regulators and identified significantly enriched Gene Ontology (GO) and Kyoto Encyclopedia of Genes and Genomes (KEGG) sets at $P < 0.05$. In the realm of biological processes, there was an enrichment of gene sets related to the assembly of mitochondrial respiratory chain complexes, particularly complex I. Analysis of cellular components revealed significant enrichment in the mitochondrial inner membrane and the respirasome. Regarding molecular function, the categories predominantly enriched included active transmembrane transporter activity and electron transfer activity (see *Figure 2A-2C*). The KEGG enrichment analysis indicated associations of phagocytosis regulators with several diseases, prominently with Alzheimer's disease among neurodegenerative disorders (see *Figure 2D*). We hypothesize that the functions of phagocytosis regulators are interconnected with the enriched GO categories and KEGG pathways identified in ccRCC.

Identification and prognostic analysis of phagocytosis regulator genes in ccRCC

Based on TCGA-KIRC expression profile, we identified 2094 up- and 2174 down-regulated genes (fold-change > 1.5 , FDR < 0.05), of which 18 were up- and 17 were down-regulated phagocytosis regulators (*Figure 3*). To ascertain their prognostic significance, we performed univariate Cox regression analyses on these phagocytosis regulator factors. This analysis identified 18 candidates with prognostic value at a $P < 0.05$ level (*Figure 4*). The Kaplan-Meier curves for the four most significant candidate genes—*POU2F2*, *QPCTL*, *KLF6*, and *SLC39A9*—indicate that they are capable of effectively distinguishing survival rates, suggesting that these genes may serve as potential

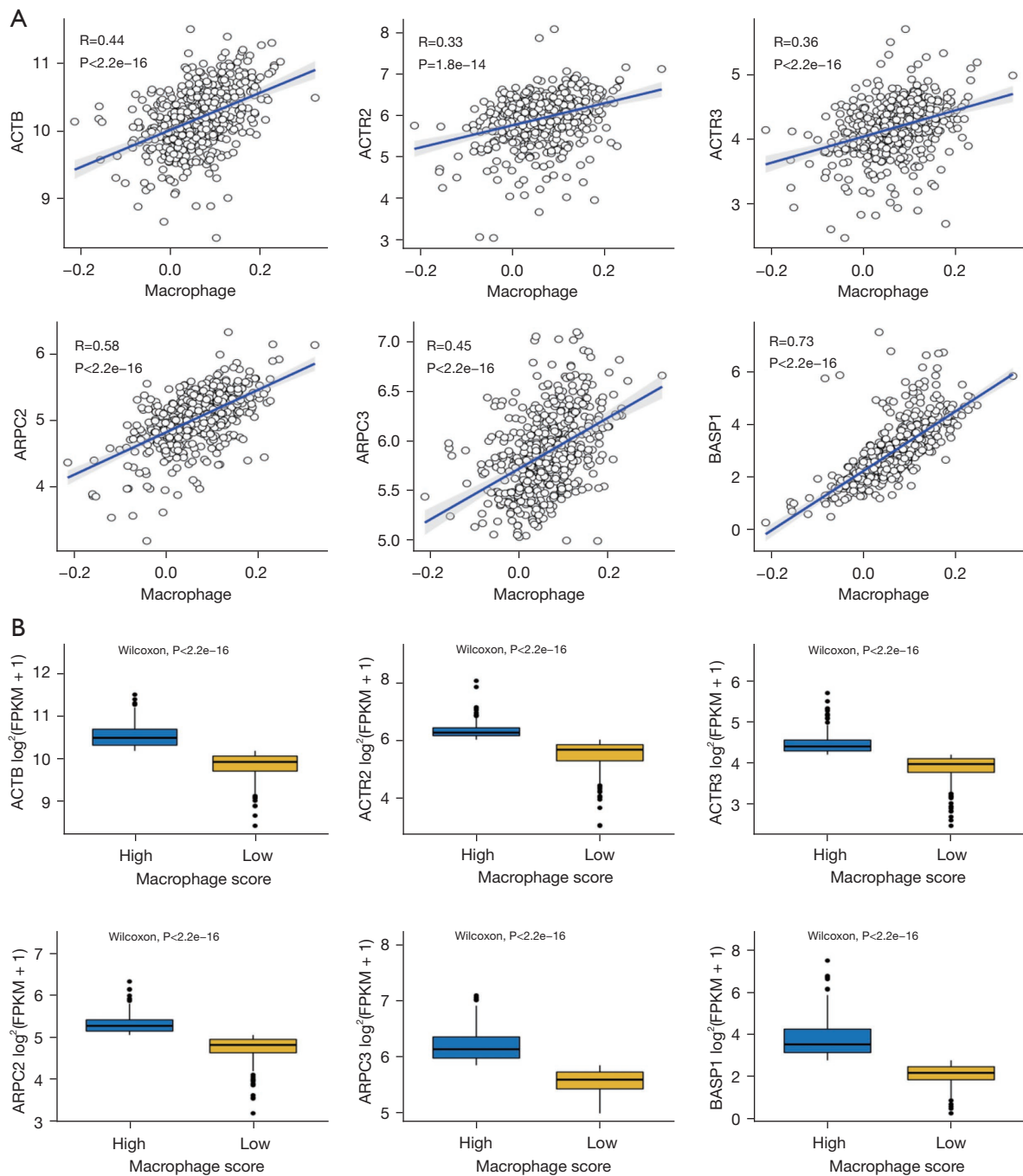


Figure 1 Association analysis of phagocytosis regulator gene expression and phagocyte ssGSEA score. Calculating the Pearson correlation between TCGA-KIRC phagocytosis gene expression and ssGSEA score of the phagocytosis regulator, the top six factors with the highest correlation are displayed with scatter plots and box plots, respectively. The horizontal axis of the scatter plot in panel A represents the ssGSEA score of macrophages, and the vertical axis is the expression of phagocytosis regulators; the boxplot in panel B divides the macrophage scores into high and low groups by the median value and uses the Mann-Whitney U test to evaluate phagocytosis differences in the expression of action regulators between the two groups. ssGSEA, single-sample gene set enrichment analysis; TCGA-KIRC, The Cancer Genome Atlas Kidney Renal Clear Cell Carcinoma.

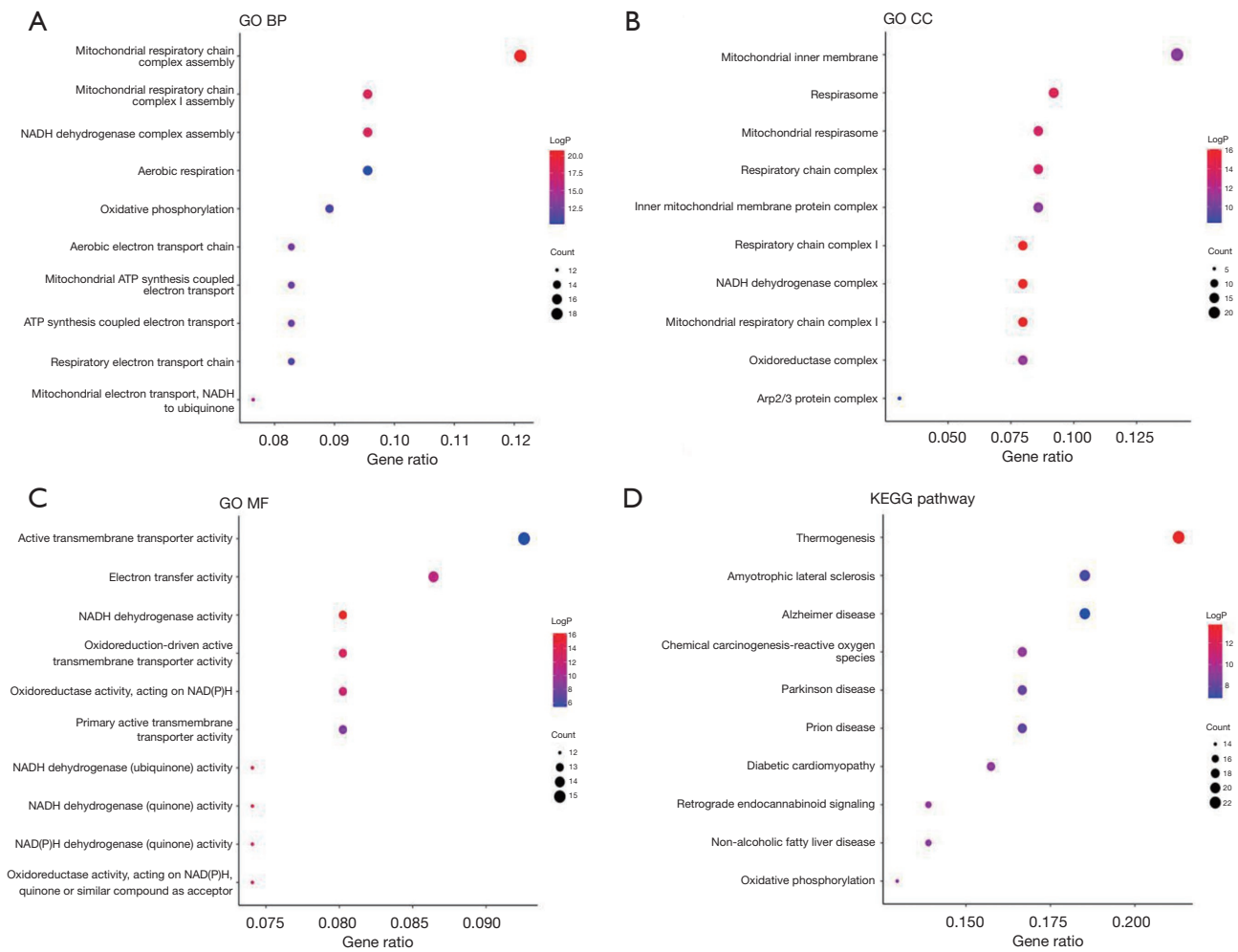


Figure 2 Functional enrichment analysis of regulators of phagocytosis. The top ten GO and KEGG functions and pathways with the highest statistical significance are displayed in the figure, respectively. Among them, each figure illustrates the top ten functions or pathways with significant results. Figure (A) shows the results of GO BP, Figure (B) reveals the results of GO CC, Figure (C) displays the results of GO MF, and Figure (D) displays KEGG results. The size of dots in the figure indicates the number of genes enriched, and the color of dots indicates the $-\log(P)$ value of statistical significance. GO, Gene Ontology; KEGG, Kyoto Encyclopedia of Genes and Genomes; BP, biological process; CC, cellular component; MF, molecular function.

biomarkers for the prognosis of ccRCC (Figure 5).

Constructing a prognostic regression model for genes related to phagocytosis regulators

Based on the prognostic candidate regulators, we used LASSO regression model for further screening (Figure 6A,6B). The remaining factors (Figure 6C) were used as phagocytosis regulatory signatures, and the following formula calculated the Signature Score: $\text{sigScore} = \sum \text{exp}i \times \text{coef}i$. Among them, i represents the prognostic

phagocytosis regulator, $\text{exp}i$ represents the expression of the factor, and coef represents the LASSO regression coefficient (Table 2).

Phagocytosis regulatory genes are associated with patient prognosis and clinical characteristics

Phagocytosis regulatory genes can predict patient prognosis

Using TCGA-KIRC as a training set for tumor prognosis

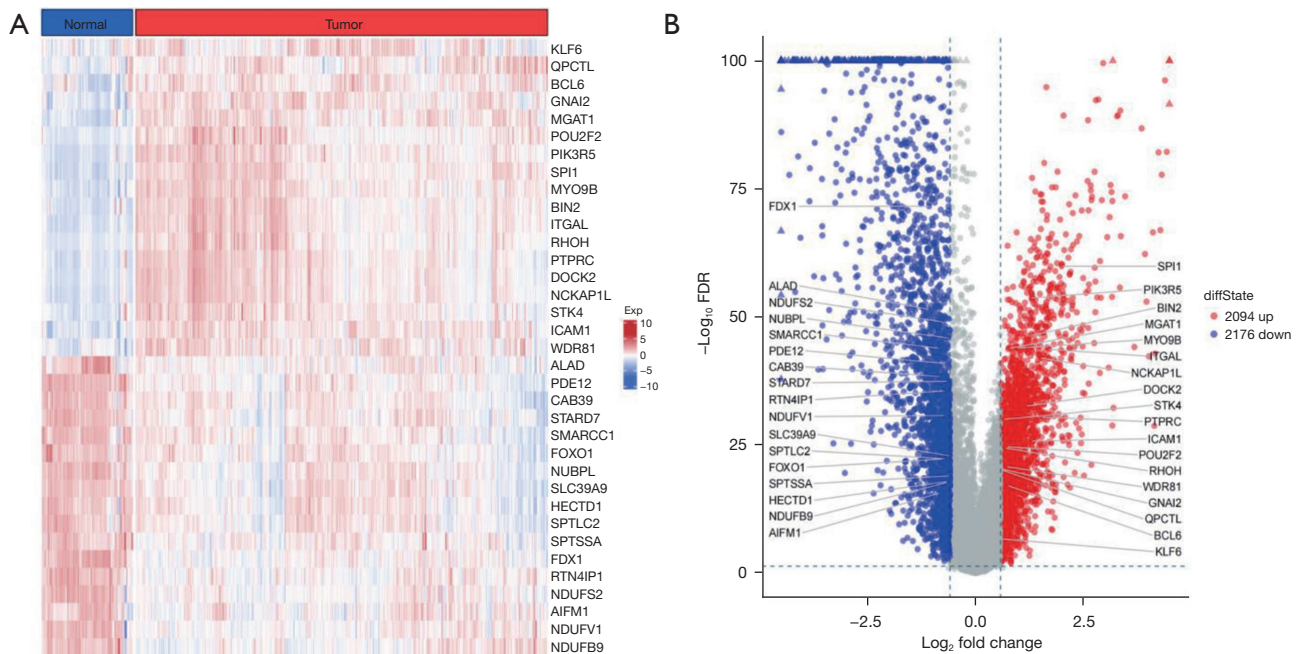


Figure 3 TCGA-KIRC identifies differentially expressed regulators of phagocytosis. The figure illustrates the heatmap (A) and the volcano plot (B) of differentially expressed phagocytosis regulators calculated by TCGA-KIRC by ImFit linear fitting model and eBayes, respectively. Among them, 18 up- and 17 down-regulated phagocytosis regulators are marked; blue surface bricks are relatively highly expressed in normal samples, and red indicates relatively high expression in tumor samples. TCGA-KIRC, The Cancer Genome Atlas Kidney Renal Clear Cell Carcinoma; FDR, false discovery rate.

of phagocytosis regulatory genes and GSE167573 as a validation set, samples were divided into two groups with high and low scores according to the median sigScore. Then, the difference in survival time between the two sample groups was evaluated. Finally, the ROC was used to evaluate phagocytosis regulation. The performance of the factor-related gene model for prognosis prediction (Figure 7, please refer to Figure S1 for the validation set). We can see that the high expression group of phagocytosis regulatory genes has a higher risk of death than the low expression group (Figure 7A). The model had a better prognostic performance at 1, 3, and 5 years with area under the curve (AUC) values of 0.747, 0.706, and 0.704, respectively (Figure 7B).

Phagocytosis regulatory genes are associated with clinical characteristics of patients

Based on the existing clinical features of the training set TCGA-KIRC and the validation set GSE167573, we compared the differences in the sigScore of different clinical feature groups (Figure 8, and the validation set is demonstrated in Figure S2). Some clinical features were

significantly correlated with phagocytosis regulatory gene scores. For example, higher tumor grade and stage levels were more likely to have higher phagocytosis regulatory genes, consistent with previous survival analysis showing phagocytosis regulators. In addition, high expression of related genes is associated with poorer prognostic risk.

Multivariate Cox regression to verify the prognostic independence of genes related to phagocytosis regulators

To test the prognostic independence of phagocytosis regulatory genes, based on the training set TCGA-KIRC and the validation set GSE167573, we performed multivariate Cox regression analysis on clinical features and sigScore grouping and found that phagocytosis regulatory genes have prognostic independence (Figure 9, see Figure S3 for the training set).

Different clinical feature groups and prognostic efficacy analyses of phagocytosis factor-related genes

To further explore the prognostic efficacy of phagocytosis

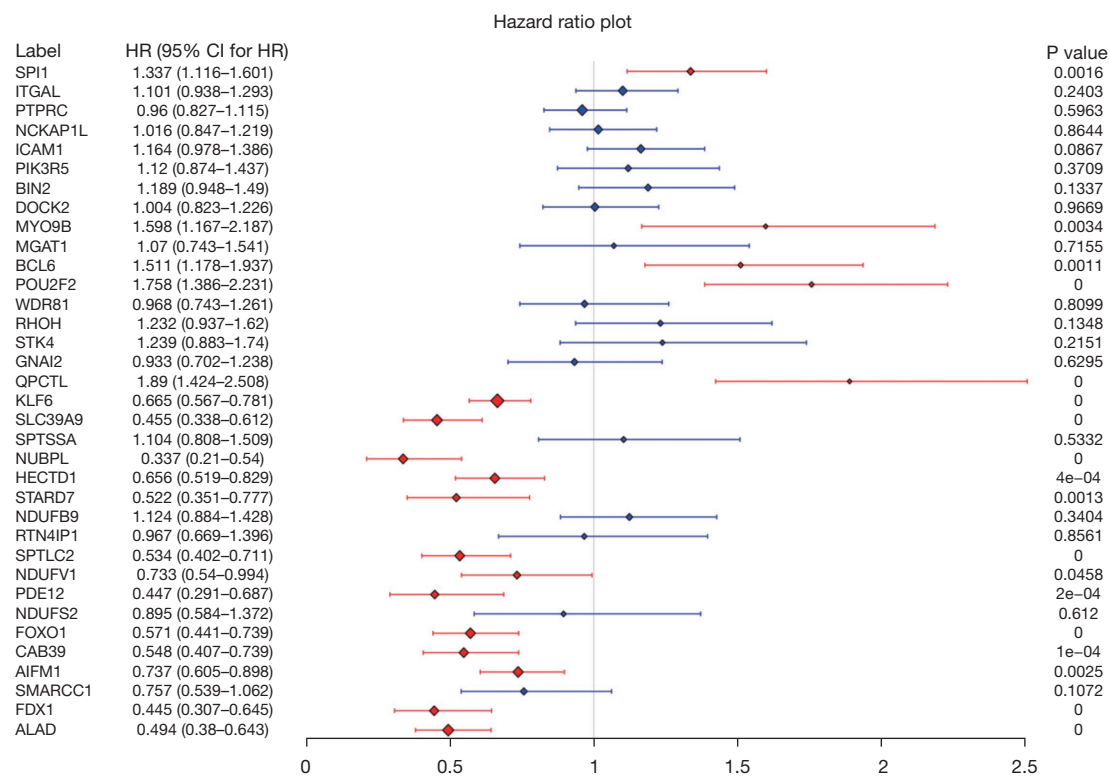


Figure 4 Forest plot of univariate Cox regression analysis of differentially expressed phagocytosis regulators. Each row in the figure demonstrates a hazard ratio boxplot for differentially expressed phagocytosis regulators, where the red boxes are risk estimates for candidate prognostic factors at $P < 0.05$ in Cox regression analysis. HR, hazard ratio; CI, confidence interval.

factor-related genes, we performed Kaplan-Meier survival analysis for different clinical feature groups and sigScore median groups of TCGA-KIRC and GSE167573 (Figure 10, and the validation set is displayed in Figure S4).

Genes related to phagocytosis regulators are related to the immune microenvironment and immunotherapy of patients

Phagocytosis regulatory genes are related to the immune microenvironment

We assessed the immune microenvironment score of TCGA-KIRC with ESTIMATE and the scores of different immune cells using various methods to investigate the association of phagocytosis regulatory genes with the immune microenvironment. We then assessed the association of phagocytosis regulatory genes with immune infiltration scores and immune cell scores (Figure 11).

The figure indicates that phagocytosis regulatory genes can significantly divide samples with different immune infiltration levels into different subgroups (Figure 11A), and sigScore has a significant positive correlation with immune infiltration scores (Figure 11B). Similarly, phagocytosis regulatory genes can significantly divide samples with different degrees of infiltration into different subpopulations based on immune cells, including macrophages (Figure 11C).

Phagocytosis regulatory genes are associated with immune checkpoints and pro-inflammatory factors

Tumor cells usually use immune checkpoint factors to “immune escape”. To further explore the association between phagocytosis signatures and macrophage immune checkpoints (22), we evaluated the relationship between each signature gene and immune checkpoint genes (Figure 12). The figure demonstrates that the high and low grouping of phagocytosis regulatory genes can significantly

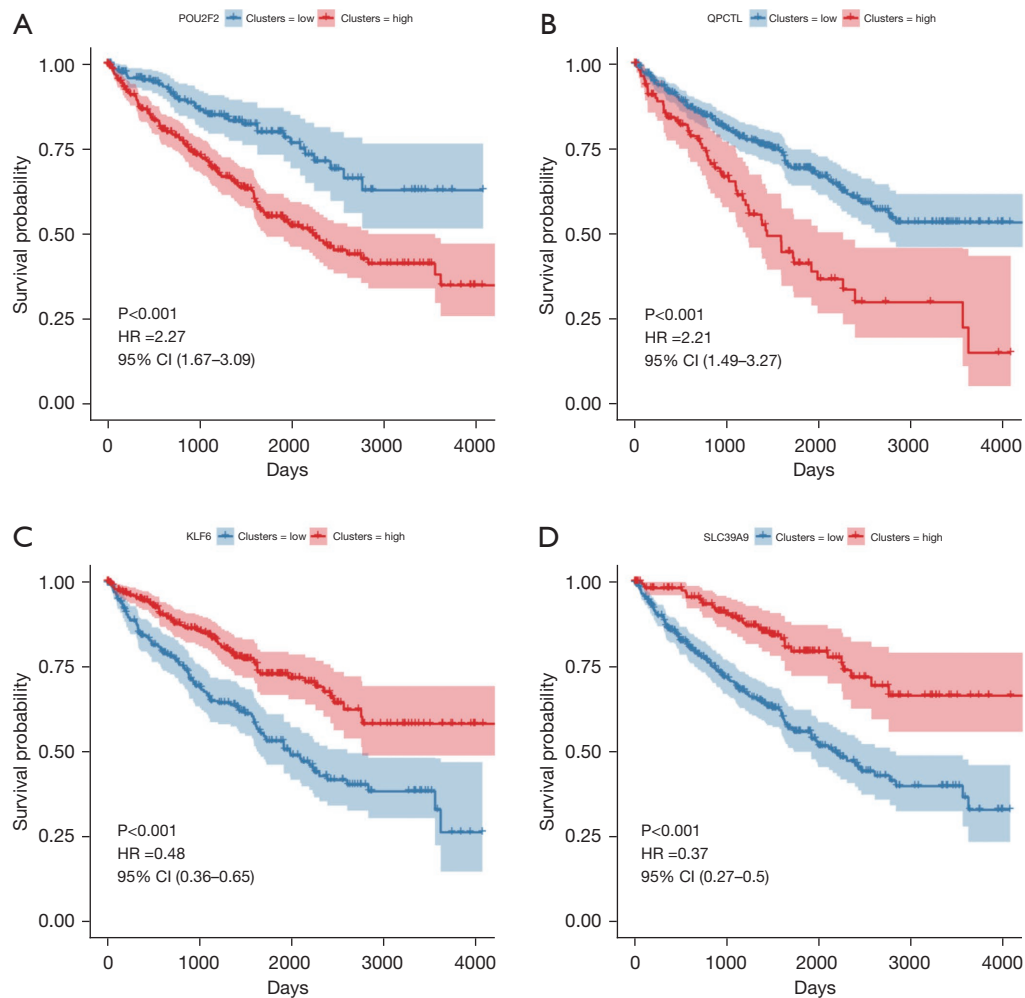


Figure 5 Kaplan-Meier curves of prognostic phagocytosis regulators. The figure reveals the survival analysis KM curve of the top 4 candidate prognostic factors with the greatest statistical significance in Cox regression analysis. The surv-cutpoint function of R package survminer divided TCGA-KRCC tumor samples into two groups and evaluated them with the log-rank test. From the P value of the statistical significance of the difference between the groups, the four factors can better distinguish the survival rate. Figure (A) shows *POU2F2*, Figure (B) reveals *QPCTL*, Figure (C) displays *KLF6*, and Figure (D) illustrates *SLC39A9*. HR, hazard ratio; CI, confidence interval; TCGA-KRCC, The Cancer Genome Atlas Kidney Renal Clear Cell Carcinoma; KM, Kaplan-Meier.

distinguish the expression levels of immune checkpoints. Concurrently, the genes in phagocytosis regulatory genes are not entirely consistent with their effects, which fully shows that phagocytosis is the combined effect of regulatory genes. In addition, the high and low grouping of phagocytosis regulatory genes depicted a negative relationship between immune checkpoint receptors and ligands, such as PD-1 gene *PDCD1* and PD-L1 gene *CD274* (Figure 12, more receptor-ligand relationships

(Figure S5).

Inflammation and cancer are inextricably linked. Pro-inflammatory factors can often mediate a variety of immune responses. Phagocytic M1 can secrete various cytokines to promote inflammation, while phagocytic M2 can secrete various inhibiting inflammatory responses factor (5). Therefore, we further explored the association between phagocytosis regulators, their genes, and pro-and anti-inflammatory factors (Figure 13). The figure manifests that

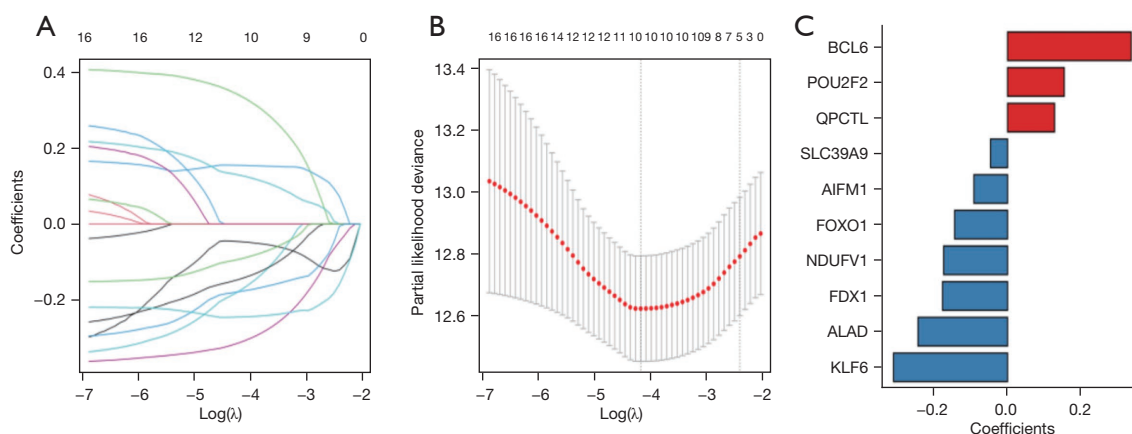


Figure 6 LASSO regression model assessing prognostic regulators of phagocytosis. Figure (A) depicts the convergence trajectory of each factor regression coefficient during the training process of LASSO regression model. Figure (B) displays that LASSO model builds 10-fold cross-validation with the minimum criteria to select the best. Figure (C) reveals the final selection of LASSO model through a bar chart of ten prognostic factors and corresponding regression coefficients. LASSO, least absolute shrinkage and selection operator.

Table 2 LASSO regressors and coefficients

Signature	Coefficients
BCL6	0.337016
POU2F2	0.154386
QPCTL	0.128073
KLF6	-0.31081
SLC39A9	-0.0464
NDUFV1	-0.17414
FOXO1	-0.1443
AIFM1	-0.09171
FDX1	-0.17718
ALAD	-0.24401

LASSO, least absolute shrinkage and selection operator.

the expression levels of corresponding genes of *IL1A*, *IL1B*, *IL-6*, *IL18*, *IL23A*, and *TNF- α* are significantly different between high and low groups of phagocytosis regulatory genes and had a consistent trend (Figure 13). The genes in phagocytosis regulators were not identical to their classification effects, fully demonstrating the combined

effect of phagocytosis regulatory genes.

Whether phagocytosis regulatory genes predict the efficacy of immunotherapy in patients

We envisioned that phagocytosis regulatory genes could predict the efficacy of immunotherapy in tumor patients. Therefore, we used a set of immunotherapy data (27) to construct a combination of phagocytosis regulatory genes in the same way as above, but the results were unsatisfactory. To this end, we tried to evaluate its performance in immunotherapy data based on the phagocytosis regulatory genes constructed by TCGA-KIRC and performed survival analysis and drug-corresponding association analysis on the collected immunotherapy data sets. Finally, a survival analysis was carried out. Unfortunately, the correlation of P values with drug response Mann-Whitney *U*'s P value is less than 0.05 to evaluate its performance, and the results are also not ideal (see Figure S6A-S6D).

Discussion

Cancer cells have long been thought to be associated with regulators of phagocytosis. However, the prognostic value of related genes in ccRCC is unclear. In our study,

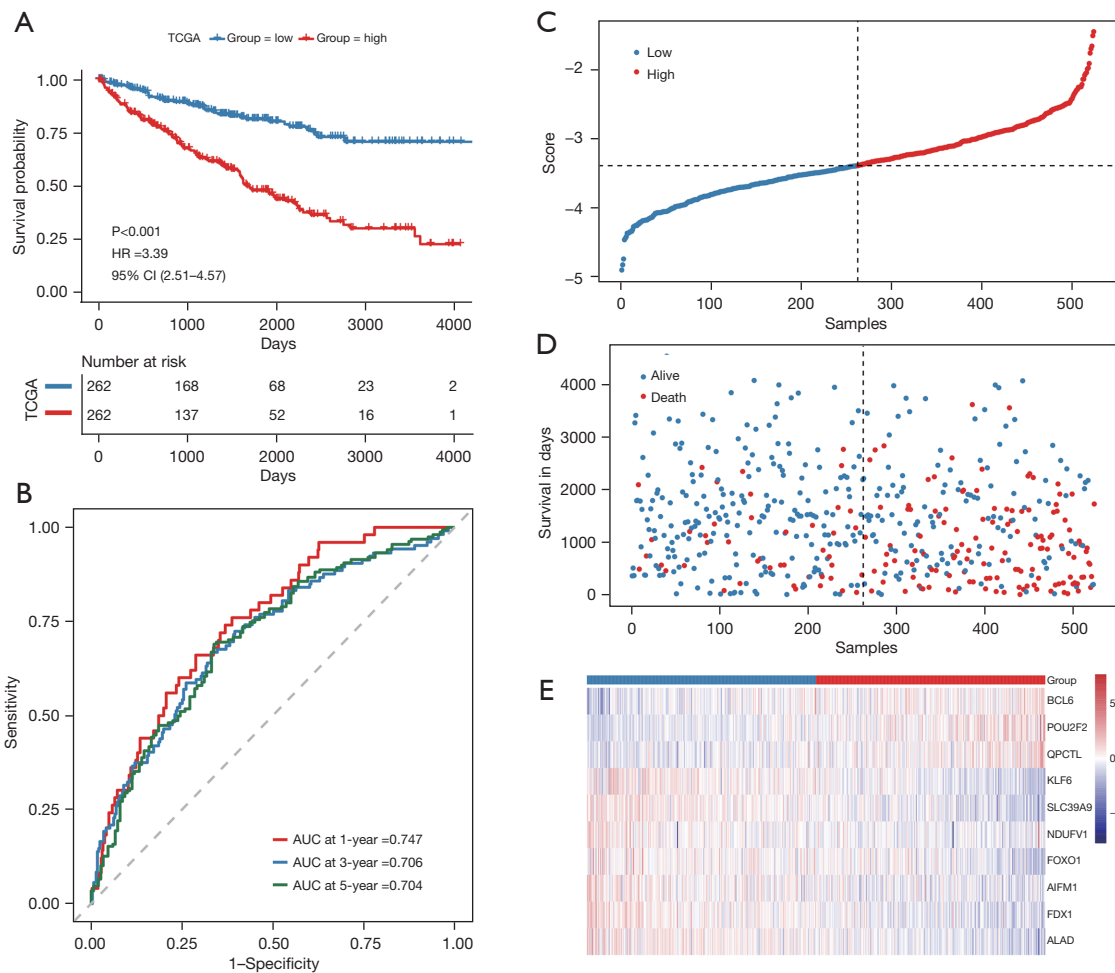


Figure 7 Training set TCGA-KIRC to assess the prognostic performance of phagocytosis-related genes. Figure (A) shows the KM survival curve of the sigScore high and low group (median grouping). Figure (B) displays ROC curve of the predictive performance of the phagocytosis regulatory gene model. Figure (C) reveals the sigScore ranking of samples from small to large. Figure (D) depicts the corresponding survival time and survival status according to the sample sorting of sigScore. Figure E displays the expression heatmap of phagocytosis regulatory genes. The gene expression levels of regulatory genes in high and low groups have a certain level of expression in the aggregation. HR, hazard ratio; CI, confidence interval; TCGA-KIRC, The Cancer Genome Atlas Kidney Renal Clear Cell Carcinoma; KM, Kaplan-Meier; ROC, receiver operating characteristic.

we investigated the relationship between phagocytosis regulatory gene expression and the prognosis of ccRCC patients in The Cancer Genome Atlas (TCGA) database. Importantly, for the first time, we attempted to construct a prognostic model of a combination of genes associated with phagocytosis regulators using LASSO Cox regression

analysis of genes. Kaplan-Meier analysis demonstrated that our model could effectively predict prognosis in TCGA-KIRC cohort and the Clinical Proteomics Cancer Analysis Consortium (cptac_ccrCC) cohort. We found that the model had optimal performance in predicting long-term survival through time-dependent ROC analysis, and

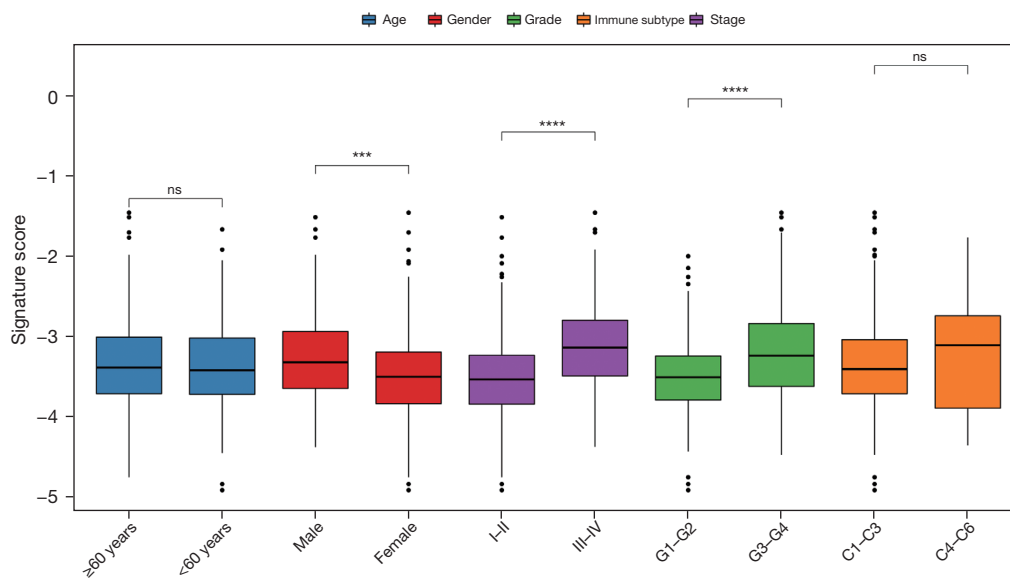


Figure 8 sigScore comparison of the training set TCGA-KIRC grouped by clinical features. The figure contains five clinical features: age (≥ 60 , < 60 years), gender (male, female), stage (I–II, III–IV), grade (G1–G2, G3–G4), and immune subtype (C1–C3, C4–C6). ***, $P < 0.001$; ****, $P < 0.0001$; ns, not significant. TCGA-KIRC, The Cancer Genome Atlas Kidney Renal Clear Cell Carcinoma.

Variable	N	Hazard ratio	P
Age (years)	<60	255	Reference
	≥ 60	253	1.67 (1.21, 2.30) 0.002
Gender	Female	179	Reference
	Male	329	0.84 (0.61, 1.16) 0.301
Stage	I–II	301	Reference
	III–IV	207	3.02 (2.15, 4.25) <0.001
Immune subtype	C1–C3	466	Reference
	C4–C6	42	2.35 (1.47, 3.76) <0.001
Sig score	Low	252	Reference
	High	256	2.55 (1.76, 3.68) <0.001

Figure 9 Multivariate Cox regression test for prognostic independence of phagocytosis factor-related genes. The figure depicts the results of multivariate Cox regression on the training set TCGA-KIRC. TCGA-KIRC, The Cancer Genome Atlas Kidney Renal Clear Cell Carcinoma.

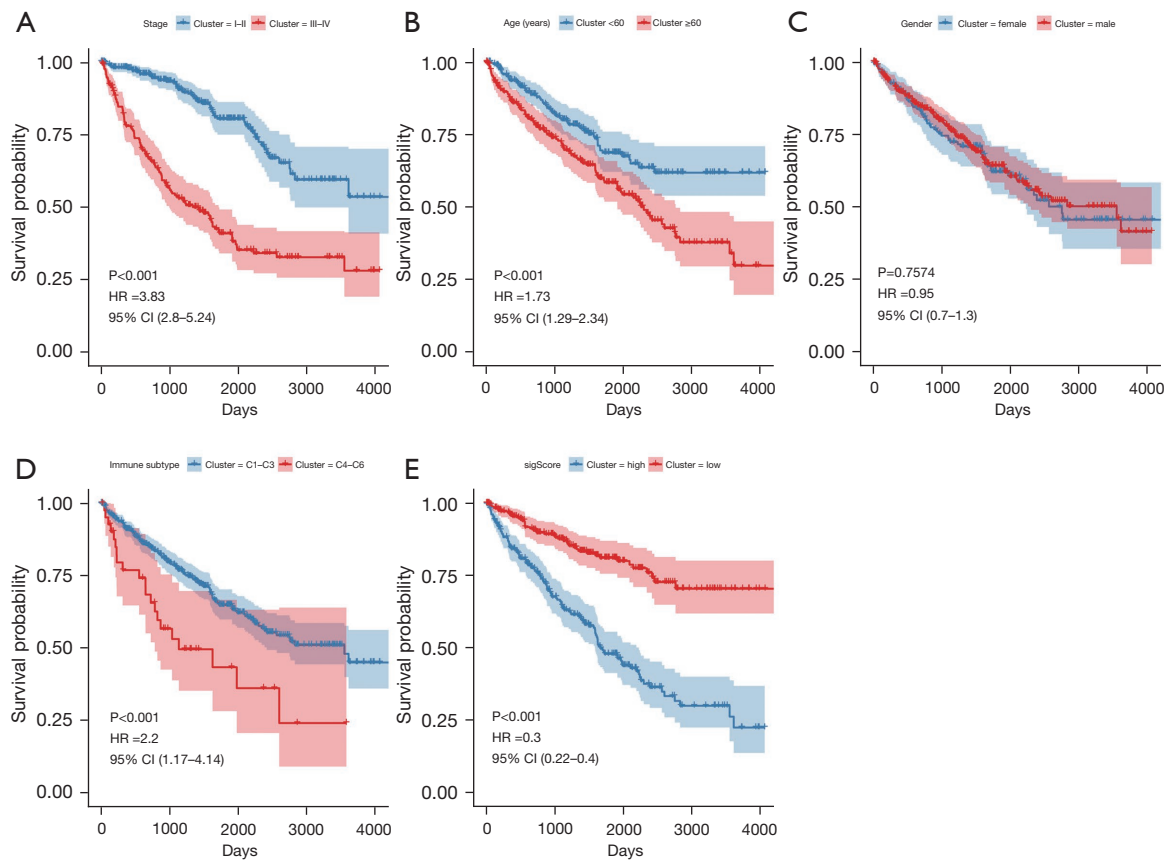


Figure 10 Kaplan-Meier survival analysis of clinical grouping versus median sigScore grouping. (A-E) The clinical characteristics of TCGA-KIRC: stage (I–II, III–IV), age (≥ 60 , < 60 years), gender (male, female), immune subtypes (C1–C3, C4–C6), and sigScore (high, low) for tumor sample grouping survival curve, log-rank test, and Cox hazard ratio. HR, hazard ratio; CI, confidence interval; TCGA-KIRC, The Cancer Genome Atlas Kidney Renal Clear Cell Carcinoma.

multivariate Cox regression analysis revealed that our combined model was an independent prognostic factor. Risk scores for each patient were significantly associated with various clinicopathological parameters. Clinical features were significantly correlated with phagocytosis regulatory gene scores. In contrast, tumors with higher levels of grade and stage were more prone to have higher phagocytosis regulatory genes, which is in contrast to previous survival analysis showing that high expression of phagocytosis

regulatory genes has poor expression. Prognostic risks echo each other. Our study suggests that phagocytosis regulatory genes do not play an ideal role in predicting the efficacy of immunotherapy in patients.

Furthermore, research by Gao *et al.* (28). has shown that KLF6 suppresses ccRCC progression by inhibiting epithelial-mesenchymal transition (EMT) and metastatic capabilities, while Wang *et al.* (29). found that POU2F2 could enhance EMT and thus promote ccRCC progression.

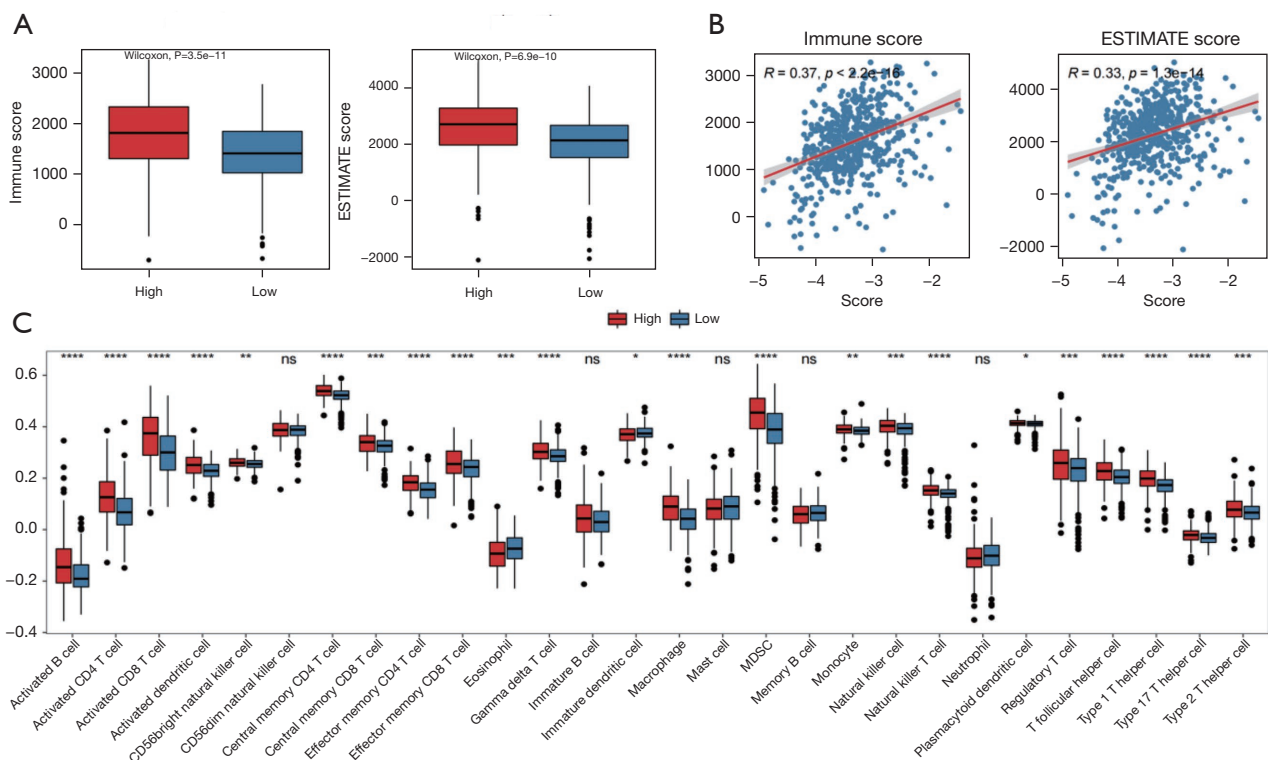


Figure 11 Correlation of phagocytosis regulatory genes with the immune microenvironment. Figure (A,B) illustrates the correlation between sigScore and TCGA-KIRC tumor immune score, and Figure (A) shows the difference between immune score and ESTIMATE score for different phagocytosis regulatory gene groupings (median value of sigScore). Figure (B) reveals the Pearson correlation of sigScore with immune score and ESTIMATE score. Figure (C) demonstrates the differences in the grouping of genes related to phagocytosis regulators for different immune cell scores, from which it can be seen that the level of phagocytic infiltration is significantly separated by sigScore. *, P<0.05; **, P<0.01; ***, P<0.001; ****, P<0.0001; ns, not significant. TCGA-KIRC, The Cancer Genome Atlas Kidney Renal Clear Cell Carcinoma.

Unlike the findings of Gao and Wang, our study uniquely identifies and confirms the regulatory roles of genes such as *POU2F2* and *KLF6* in phagocytosis, suggesting them as novel therapeutic targets. This distinction is critical as it highlights potential mechanisms by which these genes could influence tumor progression and patient survival—mechanisms previously unexplored.

Overall, our study provides new insights into the prognostic and progressive roles of phagocytosis regulatory

genes in ccRCC, expanding our understanding of their potential impact on treatment outcomes.

Conclusions

We have constructed a prognostic model of a combination of genes associated with phagocytosis regulators and provided new insights into the prognosis and progression of phagocytosis regulatory genes in ccRCC.

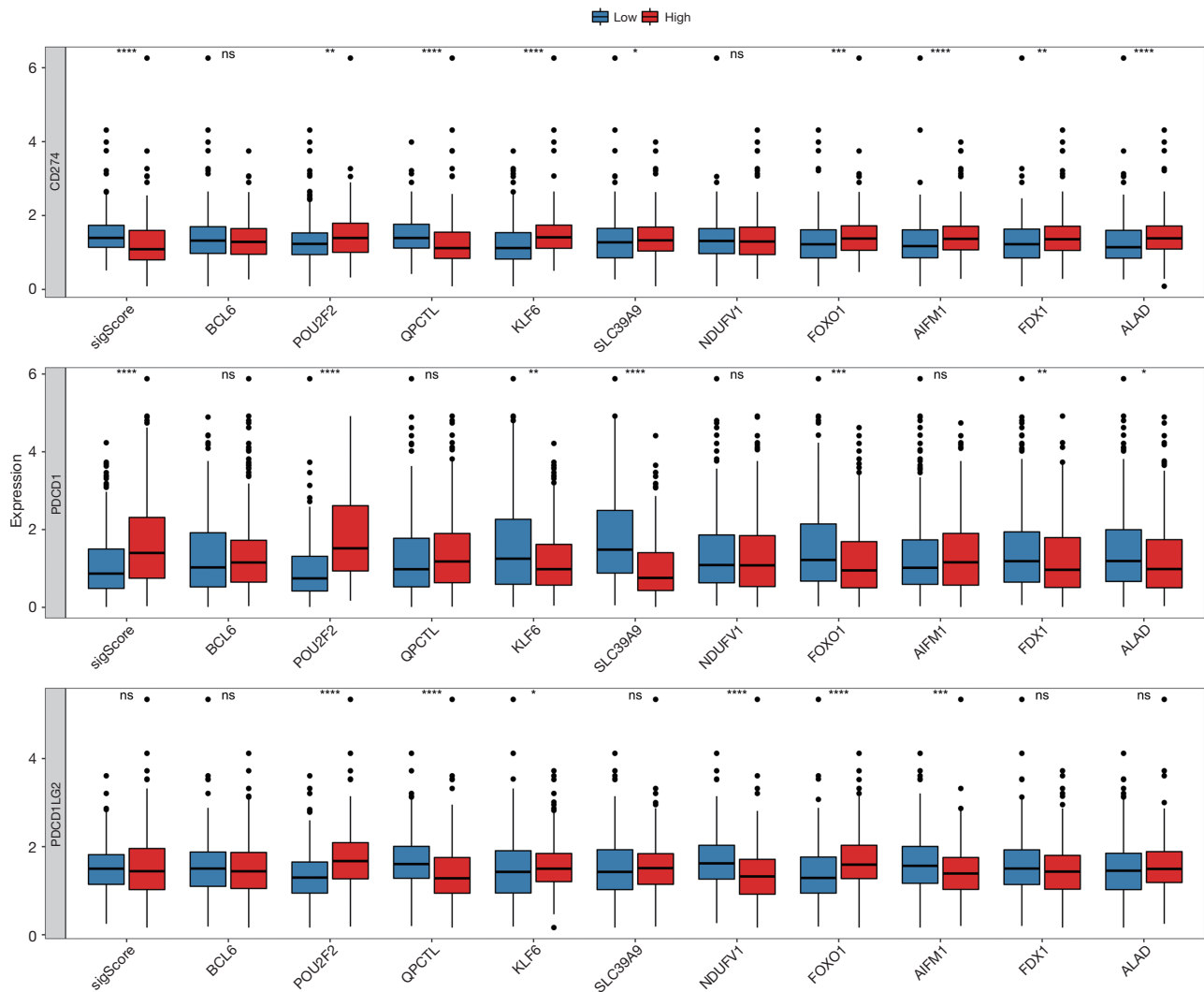


Figure 12 Association of phagocytosis regulatory genes with immune checkpoints. The sigScore and phagocytosis regulatory gene expressions were divided into high and low groups by the median value to evaluate whether the gene expression of immune checkpoints and ligands differed in different groups. The figure illustrates that the expression of the gene *PDCD1* of the immune checkpoint PD1 and the gene *CD274* of the ligand PD-L1 can be significantly grouped. *, $P < 0.05$; **, $P < 0.01$; ***, $P < 0.001$; ****, $P < 0.0001$; ns, not significant. PD-1, programmed cell death protein-1; PD-L1, programmed cell death ligand-1.

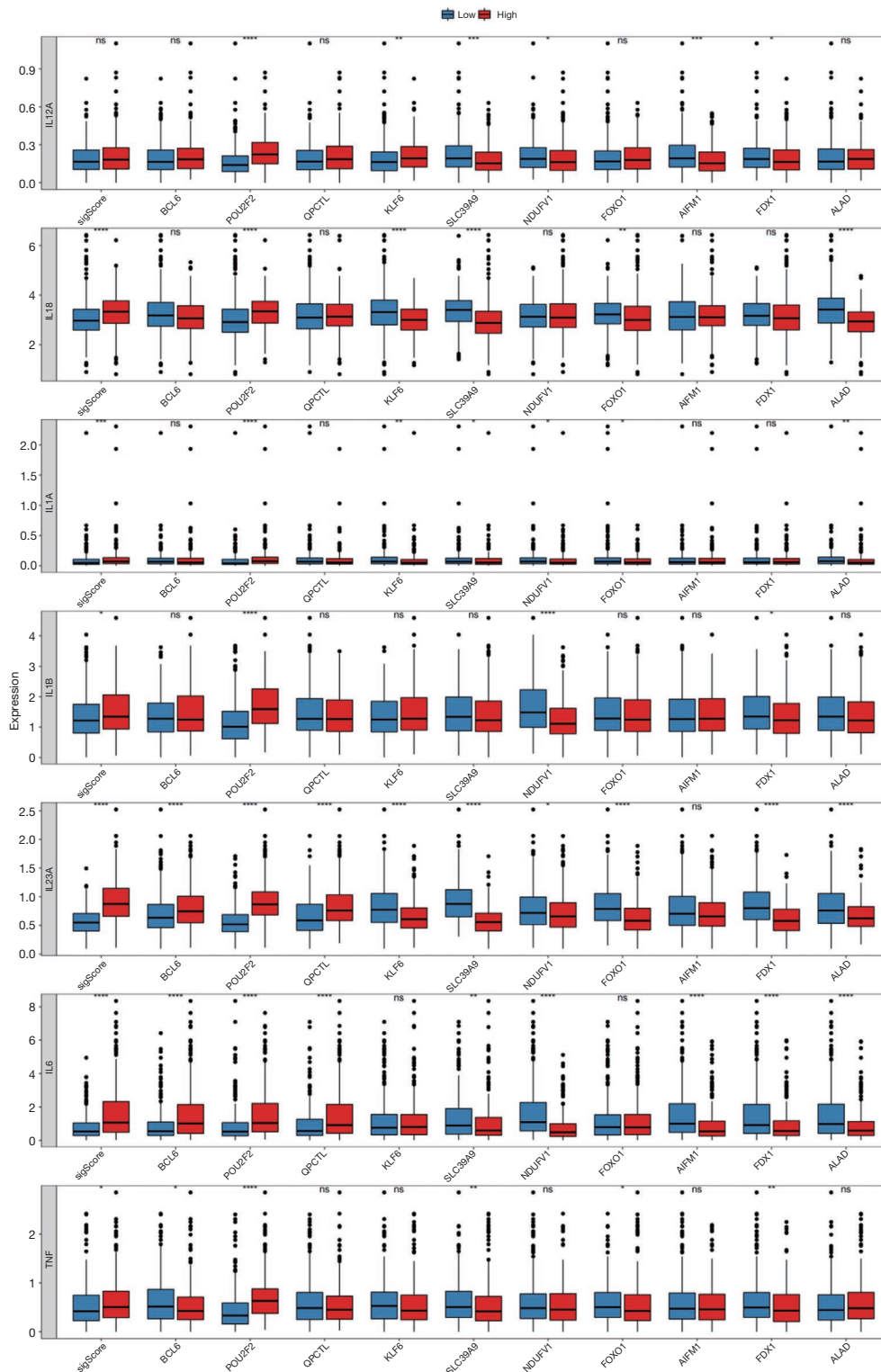


Figure 13 Signature and its gene association with pro-inflammatory factors. The figure demonstrates that the sigScore and signature gene expression is divided into two groups by the median value to evaluate the phagocyte pro-inflammatory factors *IL12A*, *IL18*, *IL1A*, *IL1B*, *IL23A*, *IL6*, and other genes in different groups and whether there is a difference in expression. *, P<0.05; **, P<0.01; ***, P<0.001; ****, P<0.0001; ns, not significant.

Acknowledgments

The authors would like to thank the public database provider in this study.

Funding: This work was supported by the Science and Technology Department of Jiangxi Province (No. 20212BAG70042).

Footnote

Reporting Checklist: The authors have completed the TRIPOD reporting checklist. Available at <https://tcr.amegrouops.com/article/view/10.21037/tcr-24-139/rc>

Peer Review File: Available at <https://tcr.amegrouops.com/article/view/10.21037/tcr-24-139/prf>

Conflicts of Interest: All authors have completed the ICMJE uniform disclosure form (available at <https://tcr.amegrouops.com/article/view/10.21037/tcr-24-139/coif>). The authors have no conflicts of interest to declare.

Ethical Statement: The authors are accountable for all aspects of the work in ensuring that questions related to the accuracy or integrity of any part of the work are appropriately investigated and resolved. The study was conducted in accordance with the Declaration of Helsinki (as revised in 2013).

Open Access Statement: This is an Open Access article distributed in accordance with the Creative Commons Attribution-NonCommercial-NoDerivs 4.0 International License (CC BY-NC-ND 4.0), which permits the non-commercial replication and distribution of the article with the strict proviso that no changes or edits are made and the original work is properly cited (including links to both the formal publication through the relevant DOI and the license). See: <https://creativecommons.org/licenses/by-nc-nd/4.0/>.

References

1. Siegel RL, Miller KD, Jemal A. Cancer statistics, 2019. *CA Cancer J Clin* 2019;69:7-34.
2. Cheng G, Liu D, Liang H, et al. A cluster of long non-coding RNAs exhibit diagnostic and prognostic values in renal cell carcinoma. *Aging (Albany NY)* 2019;11:9597-615.
3. Song Q, Shang J, Yang Z, et al. Identification of an immune signature predicting prognosis risk of patients in lung adenocarcinoma. *J Transl Med* 2019;17:70.
4. Wang Y, Ruan Z, Yu S, et al. A four-methylated mRNA signature-based risk score system predicts survival in patients with hepatocellular carcinoma. *Aging (Albany NY)* 2019;11:160-73.
5. Duan Z, Luo Y. Targeting macrophages in cancer immunotherapy. *Signal Transduct Target Ther* 2021;6:127.
6. Kamber RA, Nishiga Y, Morton B, et al. Inter-cellular CRISPR screens reveal regulators of cancer cell phagocytosis. *Nature* 2021;597:549-54.
7. Haney MS, Bohlen CJ, Morgens DW, et al. Identification of phagocytosis regulators using magnetic genome-wide CRISPR screens. *Nat Genet* 2018;50:1716-27.
8. Mantovani A, Allavena P, Sica A, et al. Cancer-related inflammation. *Nature* 2008;454:436-44.
9. Noy R, Pollard JW. Tumor-associated macrophages: from mechanisms to therapy. *Immunity* 2014;41:49-61.
10. Mantovani A, Marchesi F, Malesci A, et al. Tumour-associated macrophages as treatment targets in oncology. *Nat Rev Clin Oncol* 2017;14:399-416.
11. Morrissey MA, Kern N, Vale RD. CD47 Ligation Repositions the Inhibitory Receptor SIRPA to Suppress Integrin Activation and Phagocytosis. *Immunity* 2020;53:290-302.e6.
12. Colaprico A, Silva TC, Olsen C, et al. TCGAbiolinks: an R/Bioconductor package for integrative analysis of TCGA data. *Nucleic Acids Res* 2016;44:e71.
13. Clyde D. Cancer genomics: Keeping score with immunotherapy response. *Nat Rev Genet* 2017;18:146.
14. Thorsson V, Gibbs DL, Brown SD, et al. The Immune Landscape of Cancer. *Immunity* 2018;48:812-830.e14.
15. Hänzelmann S, Castelo R, Guinney J. GSEA: gene set variation analysis for microarray and RNA-seq data. *BMC Bioinformatics* 2013;14:7.
16. Yu G, Wang LG, Han Y, et al. clusterProfiler: an R package for comparing biological themes among gene clusters. *OMICS* 2012;16:284-7.
17. Ritchie ME, Phipson B, Wu D, et al. limma powers differential expression analyses for RNA-sequencing and microarray studies. *Nucleic Acids Res* 2015;43:e47.
18. Themeau TM, Lumley T. Package 'survival'. *R Top Doc* 2015;128:28-33.
19. Friedman J, Hastie T, Tibshirani R, et al. Package 'glmnet'. *Journal of Statistical Software*. 2010;33. Available online: <https://www.jstatsoft.org/article/view/v033i01>
20. Blanche P, Blanche M P. Package 'timeROC'. 2019. Available online: <https://cran.r-project.org/web/packages/timeROC/index.html>

21. Kennedy N. Package 'forestmodel'. Forest Plots from Regression Models. (R package version 0.6.2) 2020. Available online: <https://cran.r-project.org/web/packages/forestmodel/index.html>
22. Kassambara A, Kosinski M, Biecek P, et al. Package 'survminer'. Drawing Survival Curves using 'ggplot2'(R package version 03-1) 2017. Available online: <https://cran.r-project.org/web/packages/survminer/index.html>
23. Yoshihara K, Shahmoradgoli M, Martínez E, et al. Inferring tumour purity and stromal and immune cell admixture from expression data. *Nat Commun* 2013;4:2612.
24. Racle J, de Jonge K, Baumgaertner P, et al. Simultaneous enumeration of cancer and immune cell types from bulk tumor gene expression data. *Elife* 2017;6:e26476.
25. Finotello F, Mayer C, Plattner C, et al. Molecular and pharmacological modulators of the tumor immune contexture revealed by deconvolution of RNA-seq data. *Genome Med* 2019;11:34.
26. Zeng D, Ye Z, Shen R, et al. IOBR: Multi-Omics Immuno-Oncology Biological Research to Decode Tumor Microenvironment and Signatures. *Front Immunol* 2021;12:687975.
27. Braun DA, Hou Y, Bakouny Z, et al. Interplay of somatic alterations and immune infiltration modulates response to PD-1 blockade in advanced clear cell renal cell carcinoma. *Nat Med* 2020;26:909-18.
28. Gao Y, Li H, Ma X, et al. KLF6 Suppresses Metastasis of Clear Cell Renal Cell Carcinoma via Transcriptional Repression of E2F1. *Cancer Res* 2017;77:330-42.
29. Wang T, Wagner RT, Hlady RA, et al. SETD2 loss in renal epithelial cells drives epithelial-to-mesenchymal transition in a TGF- β -independent manner. *Mol Oncol* 2024;18:44-61.

Cite this article as: Xiao R, Luo Z, Huang H, Yin Y. Prognosis and progression of phagocytic regulatory factor-related gene combinations in clear cell renal cell carcinoma (ccRCC). *Transl Cancer Res* 2024;13(9):4878-4895. doi: 10.21037/tcr-24-139